







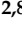




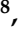






## Article

# Impact of Climate Change on Cyanobacteria Growth: A Case Study of Lama Dei Peligni Rock Paintings Conservation (Majella Massif—Abruzzo Region, Italy)

Piero Chiacchiaretta <sup>1,2</sup>, Fernanda Prestileo <sup>3,\*</sup>, Eleonora Maria Stella <sup>4</sup>, Eleonora Aruffo <sup>2,5</sup>, Pasquale Simeone <sup>2,6</sup>, Paola Lanuti <sup>2,6</sup>, Silvia Di Lodovico <sup>7</sup>, Mara Di Giulio <sup>7</sup>, Simone Guarnieri <sup>2,8</sup>, Piero Del Boccio <sup>2,5</sup>, Giorgia Spalluto <sup>2,5</sup>, Maria Concetta Cufaro <sup>1,2</sup>, Valentina Gatta <sup>2,8</sup>, Federico Anaclerio <sup>2,8</sup>, Chiara Alisi <sup>9</sup>, Stefano Dietrich <sup>3</sup>, Piero Di Carlo <sup>1,2</sup> and Alessandra Mascitelli <sup>1,2,3</sup>

- <sup>1</sup> Department of Advanced Technologies in Medicine & Dentistry, University “G. d’Annunzio” of Chieti-Pescara, 66100 Chieti, Italy; piero.chiacchiaretta@unich.it (P.C.); maria.cufaro@unich.it (M.C.C.); piero.dicarlo@unich.it (P.D.C.); alessandra.mascitelli@unich.it (A.M.)
- <sup>2</sup> Center for Advanced Studies and Technology (CAST), University “G. d’Annunzio” of Chieti-Pescara, 66100 Chieti, Italy; eleonora.aruffo@unich.it (E.A.); pasquale.simeone@unich.it (P.S.); paola.lanuti@unich.it (P.L.); simone.guarnieri@unich.it (S.G.); piero.delboccio@unich.it (P.D.B.); giorgia.spalluto@phd.unich.it (G.S.); valentina.gatta@unich.it (V.G.); federico.anaclerio@unich.it (F.A.)
- <sup>3</sup> National Research Council-Institute of Atmospheric Sciences and Climate (CNR-ISAC), Via del Fosso del Cavaliere 100, 00133 Rome, Italy; s.dietrich@isac.cnr.it
- <sup>4</sup> National Research Council-Institute of Heritage Science (CNR-ISPC), Area della Ricerca di Roma 1, Via Salaria km 29.300, 00010 Montelibretti, Italy; eleonoramaria.stella@cnr.it
- <sup>5</sup> Department of Science, University “G. d’Annunzio” of Chieti-Pescara, 66100 Chieti, Italy
- <sup>6</sup> Department of Medicine and Aging Sciences, University “G. d’Annunzio” of Chieti-Pescara, 66100 Chieti, Italy
- <sup>7</sup> Department of Pharmacy, University “G. d’Annunzio” of Chieti-Pescara, 66100 Chieti, Italy; silvia.dilodovico@unich.it (S.D.L.); mara.digiulio@unich.it (M.D.G.)
- <sup>8</sup> Department of Neuroscience, Imaging and Clinical Sciences, University “G. d’Annunzio” of Chieti-Pescara, 66100 Chieti, Italy
- <sup>9</sup> Department of Environment, Global Change and Sustainable Development, National Agency for New Technologies, Energy and Sustainable Economic Development, ENEA, 00123 Rome, Italy; chiara.alisi@enea.it
- \* Correspondence: fernanda.prestileo@cnr.it



Academic Editors: Matthias Ripp, Christer Gustafsson and Rohit Jigyasu

Received: 27 October 2025  
Revised: 19 November 2025  
Accepted: 25 November 2025  
Published: 4 December 2025

**Citation:** Chiacchiaretta, P.; Prestileo, F.; Stella, E.M.; Aruffo, E.; Simeone, P.; Lanuti, P.; Di Lodovico, S.; Di Giulio, M.; Guarnieri, S.; Del Boccio, P.; et al. Impact of Climate Change on Cyanobacteria Growth: A Case Study of Lama Dei Peligni Rock Paintings Conservation (Majella Massif—Abruzzo Region, Italy). *Sustainability* **2025**, *17*, 10861. <https://doi.org/10.3390/su172310861>

**Copyright:** © 2025 by the authors. Licensee MDPI, Basel, Switzerland. This article is an open access article distributed under the terms and conditions of the Creative Commons Attribution (CC BY) license (<https://creativecommons.org/licenses/by/4.0/>).

## Abstract

The atmosphere plays a pivotal role in modulating the interactions between microorganisms and their surrounding environments, influencing ecological cycles, heritage conservation, and providing opportunities for novel applications. Recent studies have highlighted the role of microbial responses to atmospheric conditions as indicators of environmental change. This study highlights the role of climate change, particularly rising temperatures, on the growth of cyanobacteria and, consequently, the impact of this on the conservation of cultural heritage, as in the case study of the rock paintings of the Majella Massif (Lama dei Peligni—Abruzzo Region, central Italy). The region’s rock art, characterized by red and black schematic motifs, is increasingly impacted by microbial colonization, driven by climate-induced temperature variations. These impacts are consistent with broader research demonstrating the link between microbial growth patterns and climatic factors. Laboratory analyses were carried out on cyanobacteria samples collected near the rock paintings at the study site in the Majella National Park. Results revealed a significant increase in growth rates at the higher temperature, demonstrating their sensitivity to climatic shifts. These findings underscore the dynamic role of atmospheric factors in shaping microbial survival and propagation. Consequently, certain atmospheric parameters appear to play a crucial role in the deterioration of fragile cultural assets. Indeed, the enhanced growth of cyanobacteria due to rising temperatures also poses a challenge: their proliferation can

degrade cultural heritage sites, threatening their preservation. This research advocates for interdisciplinary approaches that integrate atmospheric sciences, microbial ecology, and heritage studies to explore the role of temperature in affecting cyanobacteria growth and the conservation of a peculiar cultural heritage in the Majella Massif. By leveraging their biological traits, cyanobacteria can provide valuable insights into climate dynamics while emphasizing the urgency for proactive strategies to mitigate environmental impacts on vulnerable ecosystems and heritage sites.

**Keywords:** climate change; temperature; cyanobacteria; rock paintings; cultural heritage; atmosphere

## 1. Introduction

In the territories of the Maiella National Park there is the highest concentration of examples of rock art of the entire Italian Apennines Mountain chain [1]. This local heritage has increased over the last decades as a result of important discoveries. The largest catalogue [2] on the rock art of central Italy provides a first chronological and typological picture of over 30 sites documented in Abruzzo Region (Italy), placing it in the ambit of the post-paleolithic schematic art of the Mediterranean. Numerous testimonies have been found in a rather limited location. In fact, thanks to the investigations carried out since 2006, the panorama of prehistoric rock art sites in the valleys of Sangro and Aventino river (Chieti province) has greatly expanded. This extraordinary concentration of sites that have similar characteristics but also important differences has allowed us to start a systematic methodological approach for the interpretation of these sites, their environmental contexts and the recurring themes of their representations [3]. The dating and frequenting of the places can be traced back to the late Bronze Age and/or early Iron Age [4]. The black and red paintings (and engravings) include anthropomorphic motifs but mainly geometric and irregular patterns. The three sites of Civitaluparella and the site of Fallo (Chieti) have similarities also under the iconographic profile being united by a recurring symbol of extreme significance: the crusader circle, a stylized representation of the sun. All of these sites are located in inaccessible locations; the small space available suggests, in fact, that they were designed for initiatory rites for a few people. In some cases, the natural characteristics of the places and the proximity of the sites, suggest the presence of ceremonial landscapes (a kind of ritual path) as their possible interpretation. Specifically, in this study, we focused on the difficult-to-reach site of “Riparo La Pineta” (La Pineta shelter) at Lama dei Peligni ( $\varphi$ : 42°03' N;  $\lambda$ : 14°11' E; H: 669 m a.s.l.) (Figure 1).

In this site, already included in the census by Mattioli in 2007 [2,5] but not investigated, there is evidence of red anthropomorphic motifs paintings (Figure 2a). These red paintings are covered in some areas by a black biofilm which alters the appearance of surfaces (Figure 2b). The growth of peculiar biological organisms on stone surfaces are due both to environmental parameters (such as temperature, relative humidity, lighting conditions, atmospheric pollution, wind and rainfall) and to the nature and properties of the stone itself (such as mineral composition, pH, ratio of various minerals, salinity, content of moisture and consistency). Therefore, the ecological and physiological requirements of the biological species involved determine the response of organisms to a colonizing surface [6–8]. There is a wide range of literature from recent decades on the fundamental role that biological agents play in the deterioration of stones. By now, it is well established that the microbiota on stone represents a complex ecosystem capable of developing in multiple ways, depending on the environmental conditions and the physical–chemical properties

of the specific material. The process of stone colonisation is accelerated by the complex chemical–physical interaction of atmospheric pollutants with the mineral material [9–18]. The availability of light, water and nutrients affects the biodeterioration of exposed stone surfaces. Thanks to the biosolubilisation of limestone, microorganisms get the various elements they need for their metabolism (such as calcium, aluminium, silicon, iron and potassium). The result of the biosolubilisation process is the production of different organic and inorganic acids by the micro-organisms [6,12]. The first colonisers of stone surfaces are algae and cyanobacteria, as their photosynthetic nature causes chemical as well as mechanical deterioration. The microclimate determines the degree of colonization, the type of community and its specific composition [19]. Their presence can be detected through the patinas or crusts they form [6,13]. The cyanobacteria can grow as subaerial biofilms that may have several colours (white, red, blue, and black), complex communities adhering to a surface and facing the atmosphere [20,21]. They are crucial to the ecology of many different habitats [22,23]. The characteristics that influence the colonisation of surfaces by cyanobacteria, determining the bioreceptivity, are varied [24,25]. These characteristics include surface roughness and lithotype of stone [19,24,26], angle of inclination, geometry of surface and shadow degree [19,27–29]. The cyanobacteria are adaptive to the light quality by modifying their pigmentation or their photosynthesis. Light therefore represents a determining factor in niche differentiation in natural environments [30,31]. Furthermore, these subaerial biofilm can serve as a substrate for the growth of further deterioration agents. In association, both these agents and the cyanobacteria can produce aesthetic, chemical and physical deterioration that compromises material durability [11]. As highlighted by Macedo et al. 2009 [19], reviewing studies conducted since the 1990s, in the Mediterranean basin (Mediterranean climate), the most common taxa found on stone cultural heritage include *Gloeocapsa*, *Phormidium* and *Chroococcus* for cyanobacteria, and *Chlorella*, *Stichococcus* and *Chlorococcum* for chlorophytes. These genera have been observed to be associated with all lithotypes (siliceous or calcareous). The preference of cyanobacteria and chlorophytes for a specific stone substrate is not easy to correlate immediately. The data examined suggest that green algae and cyanobacteria can colonise a wide variety of substrates. In the complex set of factors mentioned above, in many cases it is not always easy to evaluate the influence of each of them individually; assessing their combined effects, synergy and dynamics is complex, and all factors are likely to be significant. These biofilms can have a dual role on stone, oscillating between bioprotection and biodeterioration, based on the surrounding environment. On a case-by-case basis, biodeterioration and bioprotection must be assessed comprehensively and quantitatively, taking into account the active and dominant species, the specific lithic matrix, environmental conditions, etc. [32]. In addition, different perceptions of issues related to biodeterioration are generally influenced by the feature surface of cultural heritage concerned (a statue, a fountain, a building, a façade, an archaeological site, etc.) and on local cultural tradition [33]. In general, however, any covering caused by micro-organisms detracts from the original appearance of the heritage site. Therefore, conservators of stone heritage located outdoors, especially in the Latin cultural area, consider it a priority to keep all stone heritage surfaces clean (i.e., free of biological patina) and manage conservation plans accordingly [33]. Restoration interventions usually involve devitalisation and mechanical removal of microbial biofilms and lichen thalli [34]. Synthetic chemicals such as biocides, which have been used for decades, are now increasingly considered environmentally unsustainable. Therefore, in order to control biological growth, the research is currently focused on developing alternative products and/or approaches that do not involve the use of chemicals [35,36]. Recent studies have highlighted the role of microbial responses to atmospheric conditions as indicators of environmental change [37,38]. Although it has been demonstrated that local climatic con-

ditions influence the microbial population and community on stone, comparative studies on this microbiome in a variety of climatic conditions are very limited, hindering a better comprehension of this subject of research [39–43]. In line with this, the performed study includes an interdisciplinary analysis that integrate atmospheric sciences, microbial ecology, and heritage studies to evaluate the role of temperature in affecting cyanobacteria growth and the conservation of a peculiar cultural heritage in the Majella Massif. The impact of climate change in this area (Abruzzo Region, Italy) has shown clear variations in terms of the atmospheric mean temperature. In this study, the effect of this parameter on the growth of bacteria responsible for the black patina has been evaluated, using the Majella Massif region of Central Italy as a case study. These impacts align with broader research showing the link between microbial growth patterns and climatic factors [38,44–47].

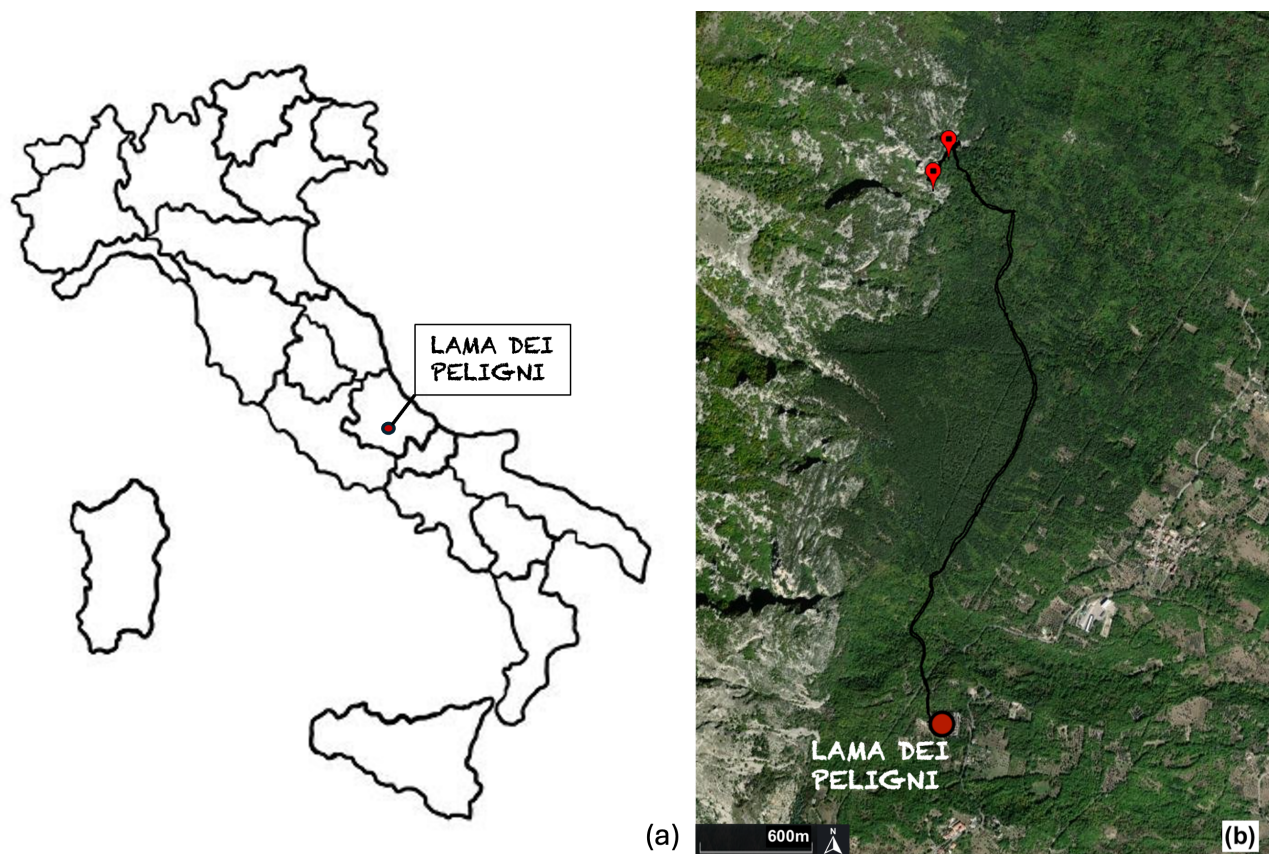


**Figure 1.** (a) Site location in Lama dei Peligni, Abruzzo Region—Central Italy. (b) Map (Google Earth Image © 2025) of site location (two red markers) in relation to the town center of Lama dei Peligni (red circle marker) and route to reach the site of interest (black line).

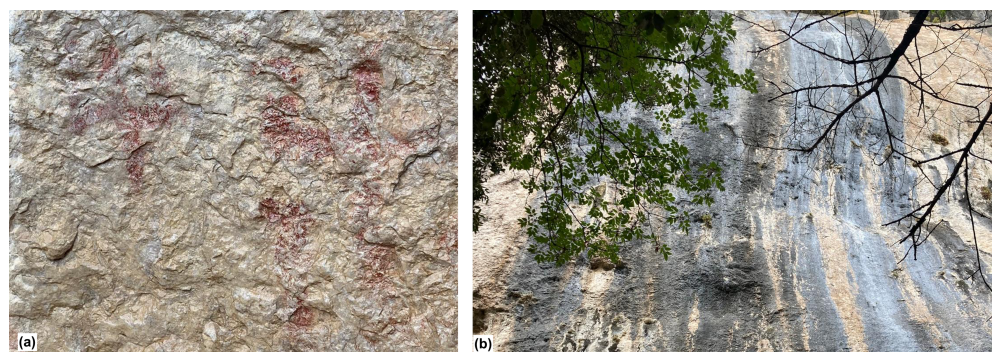


**Figure 2.** (a) One of red anthropomorphic motifs paintings located in the site of interest. (b) Black biofilm which alters the appearance of surfaces in some areas (photos by A. Mascitelli, 2024).

## 2. Materials and Methods

### 2.1. Research Design

Within the Majella National Park (Figure 3), there is the highest density of rock art currently known along the Italian Apennine chain. This great cultural heritage is well documented by large catalogues (see Section 1), placing Abruzzo Region in the range of the post-paleolithic schematic art of the Mediterranean. In this framework, at the Lama dei Peligni (Abruzzo) site, black stripes are affecting and covering the listed red rock paintings. In order to assess their origin and any actions that could mitigate their effects on the paintings, two samples (21 May 2024 and 10 July 2024) were taken (Figure 3) with the goal of conducting dedicated laboratory analyses (see Section 2.3), which revealed the presence of organic (i.e., cyanobacteria [48]) and inorganic substance (see Section 3). Samples were taken using a scalpel and sterile test tubes and swabs. Tests related to the average atmospheric temperature (see Section 2.2) were performed. Laboratory analysis, detecting the presence of cyanobacteria biofilms in proximity to the rock paintings, led to start to growth tests, which were carried out in comparison to the average atmospheric temperature. These tests aim to show the role of increasing temperature in the in the development of cyanobacteria (see Section 3).

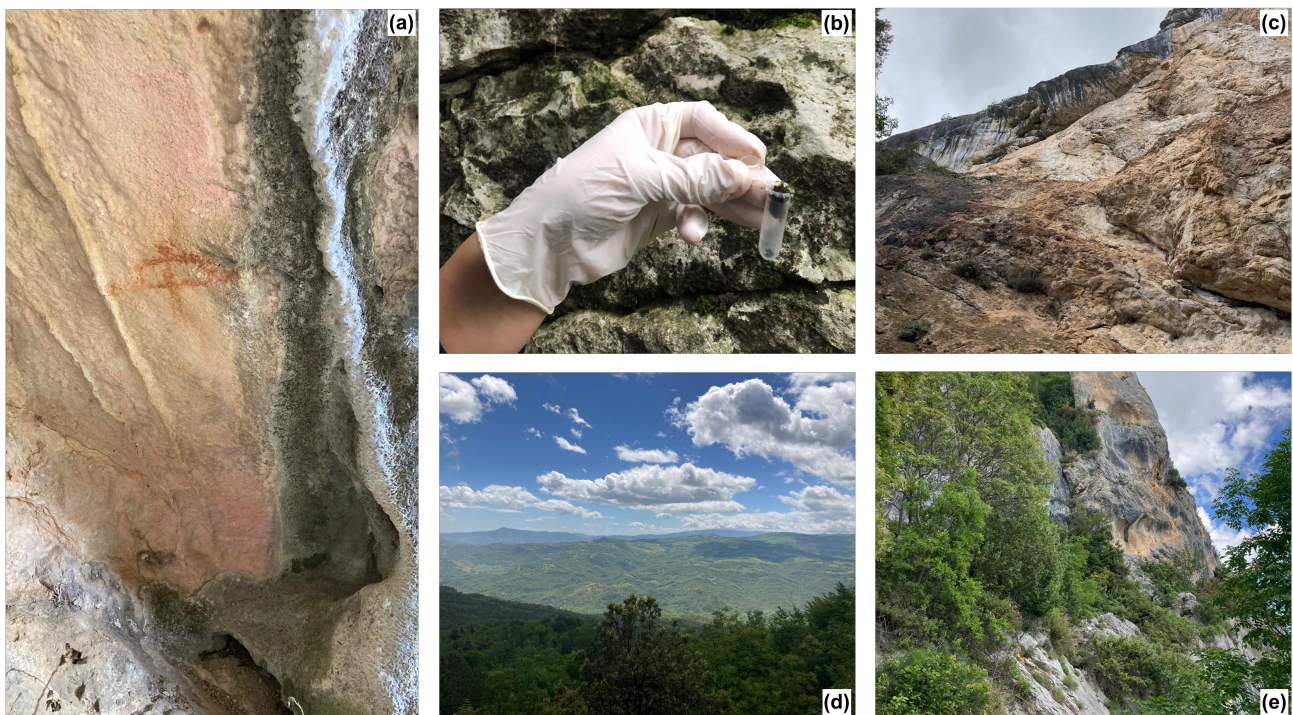


**Figure 3.** (a) One of red anthropomorphic motifs paintings close to a black stripe. (b) Sample collection. (c–e) Views of the area (photos by A. Mascitelli, 2024).

### 2.2. Atmospheric Analysis

Meteorological data are provided by the Regional Hydrographic Office. We accessed temperature data spanning from 1930 to 2023 for the Palena and Lama dei Peligni site stations (Figure 4). In this research, we applied a quality check that evaluated potential anomalies such as missing data or spikes. Two temperatures were selected for the tests: an average of the maximum temperatures for the period 1930–1970 at the Palena site (14.3 °C), the closest station ( $\approx 7.5$  km) to the Lama dei Peligni site for which data were available, and an average of the maximum temperatures for the year 2023 at the Lama dei Peligni site (18.6 °C).

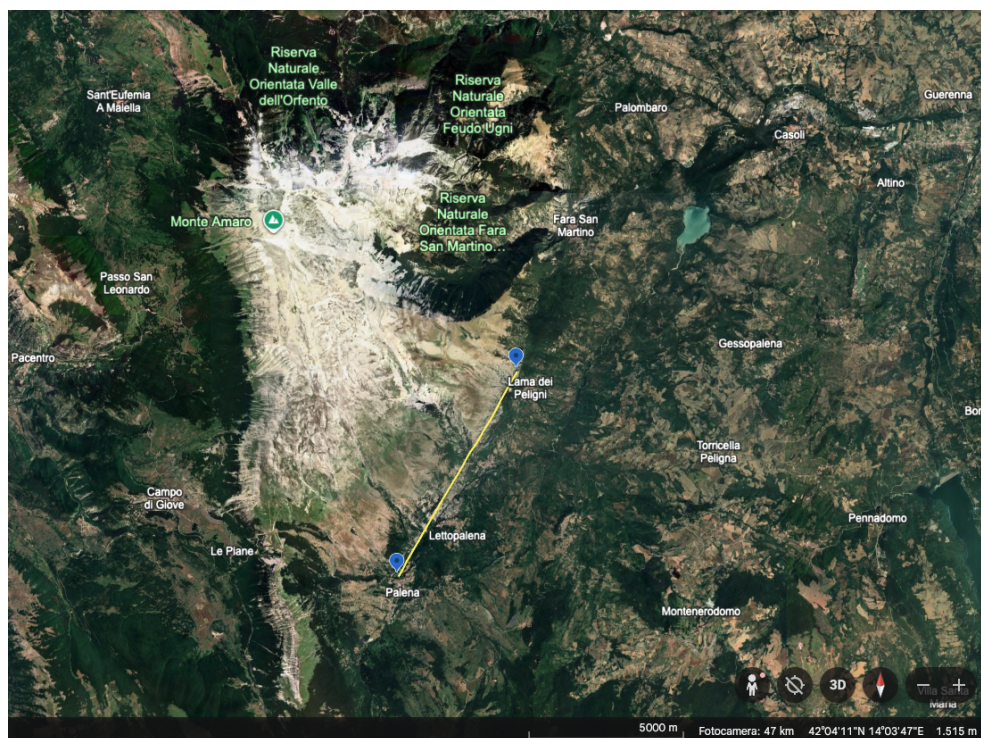


**Figure 4.** Map (Google Earth Image © 2025) of Palena and Lama dei Peligni site stations (light-blue markers) and the distance between them (yellow line  $\approx$  7.5 km).

### 2.3. Laboratory Tests

Laboratory tests were performed to classify the different components of the biofilm samples and identify the cyanobacteria, with the aim of assessing their growth in relation to temperature variations linked to climate change in the area of interest. After the classification, as reported below, the collected samples have been analysed at two selected temperatures: 14.3 °C and 18.6 °C (see Section 2.2). The culture medium used was BG11 plus 1.2% of agar bacteriological to isolate the bacterial colonies. Plates were incubated at the two temperatures up to four weeks and exposed at natural light/darkness cycles [49,50]. For the sake of clarity, the analytical procedure is shown below in Figure 5.

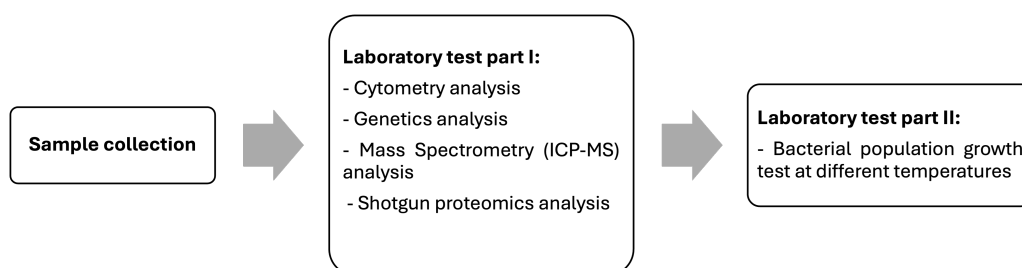


**Figure 5.** Flow chart of analytical procedure.

#### 2.3.1. Cytometry Analysis

Bacterial samples collected by sterile swabs were analyzed by flow cytometry. Briefly,  $1 \times 10^6$  cells per sample were stained with SYTO9 at a final concentration of 5  $\mu$ M (Invitrogen, ThermoFisher Scientific, Waltham, MA, USA) and incubated for 30 min at room temperature in the dark. After incubation, the samples were washed, and at least 20,000 events per sample were acquired using either a FACSVerse™ flow cytometer or a FACSARIA™ III cell sorter (both from BD Biosciences, San Jose, CA, USA). A trigger threshold was used on the FITC channel (SYTO9 emission) to exclude all non-nucleated events. Fluorescence minus one (FMO) controls were used to identify positive populations. Both FACSVerse and FACSARIA III used for flow cytometric analyses were equipped with a 633 nm red laser, and

instrument performance and quality control were verified prior to each acquisition using the BD Cytometer Setup & Tracking (CS&T) system (Becton Dickinson, Franklin Lakes, NJ, USA). Because the aim of the analysis was the qualitative identification and separation of cyanobacteria based on their intrinsic autofluorescence, the measurements did not yield quantitative data, and therefore, an intra-assay coefficient of variation was not calculated. Furthermore, given that cyanobacteria exhibit an emission peak around 650–660 nm, cells (SYTO9+ events) emitting in the Alexa Fluor 647 channel (660/20 nm) were isolated by cell sorting using a 100 µm nozzle. Those cells were further cultured.

### 2.3.2. Genetics Analysis

Bacterial DNA was isolated from the environmental samples using the Magpurix system together with the Bacterial DNA Extraction Kit (Zinexts Life Science Corp., Taipei, Taiwan, Cat. ZP02006), following the protocol supplied by the manufacturer. To monitor data quality throughout the metagenomic workflow, both negative and positive controls were included. Blank swabs and extraction blanks served as negative controls and allowed us to identify possible sources of contamination originating from sample handling or sequencing procedures. In parallel, positive controls composed of defined microbial consortia were processed to confirm the sensitivity and overall performance of the sequencing pipeline and to validate that the detected taxa reflected genuine community members. Quantification of the extracted DNA was carried out using a Qubit 3.0 fluorometer (ThermoFisher, Waltham, MA, USA). Metagenomic sequencing was performed with the Ion 16S™ Metagenomics Kit (Thermo Fisher Scientific, Waltham, MA, USA), which is optimized for the Ion Torrent™ semiconductor technology (Ion Torrent, South San Francisco, CA, USA) and enables amplification of multiple hypervariable regions of the bacterial 16S rRNA gene. The kit employs two distinct primer mixes targeting complementary sets of 16S hypervariable regions (V2–4–8 and V3–6, 7–9), thereby broadening the taxonomic resolution attainable from mixed bacterial samples. Library concentrations were assessed with the StepOne Real-Time PCR System (Thermo Fisher Scientific), and sequencing was conducted on the Ion S5™ platform using Ion 520™ chips (Thermo Fisher Scientific, Waltham, MA, USA). Data were then processed with the Ion 16S™ metagenomics workflow integrated into Ion Reporter™ Software version 5.14, enabling rapid and semi-quantitative profiling of complex microbial communities. The primers are used in combination with Environmental Master Mix v2.0, formulated to withstand high levels of PCR inhibitors typically found in environmental, food, or tissue samples. The dual-pool design supports robust amplification and broader representation of bacterial diversity. Bioinformatic interpretation of the sequencing output was carried out with Krona Software (<https://bio.tools/krona>, accessed on 26 October 2025), which provides hierarchical visualization of taxonomic groups from higher-level phyla down to more specific phylogenetic classes.

### 2.3.3. Inductively Coupled Plasma–Mass Spectrometry (ICP-MS) Analysis

Samples of moss, blackened moss, blackened soil and rock surface were digested using acidic digestion by adding 69% (*v/v*)  $HNO_3$  at a sample-to-acid ratio of 1:2, heating at 80 °C for 3 h. After that, digested samples were diluted with high-purity water (18 MΩcm<sup>-1</sup> resistivity) to have a final concentration of 7% (*v/v*)  $HNO_3$ . The same concentration of  $HNO_3$  was used in solution standard curve (levels from 0 ng mL<sup>-1</sup> to 100 ng mL<sup>-1</sup>) using the multielement mixture (Ag, Ba, Be, Cd, Co, Cr, Cu, Fe, Mn, Ni, Pb, Rb, Se, Sr, Tl, U, V, and Zn) at 10 µg mL<sup>-1</sup> (Agilent Technologies, Santa Clara, CA, USA). Samples and calibrators were analyzed in triplicate by Inductively Coupled Plasma–Mass Spectrometry (ICP-MS) with the Agilent 7900 ICP-MS quadrupolar mass spectrometer (Agilent Technologies, Santa Clara, CA, USA). An internal standard correction was performed by online addition of

an internal standard solution of Y, Bi and In at 200  $\mu\text{g mL}^{-1}$ ) in a T-piece. In particular, some elements (Cr, Co, Se, Cu, Ni, Al, As, Cd, Pb, Zn and Tl) were acquired in helium (He) mode to reduce spectral interference and noise effects; other elements (V, Mn and Ag) were measured in no-gas mode due to the lack of interference. All specifications for ICP-MS acquisition in terms of its optimization are reported in Chiaudani et al. [51], whereas detailed instrumental parameters and operating ICP-MS conditions are detailed in Table 1.

**Table 1.** List of ICP-MS instrumentation parameters.

Instrument Parameters	
Nebulizer	Babington
Torch	Quartz glass torch
Spray chamber	Scott double-pass type at 2 °C
Sample cone Nickel	1.00 mm aperture
Skimmer cone Nickel	0.40 mm aperture
Plasma mode	Normal plasma
RF power (W)	1550
RF matching (V)	1.8
Sample depth (mm)	10
Nebulizer gas ( $\text{L min}^{-1}$ )	1.03
Nebulizer pump (rps)	0.1
Plasma gas ( $\text{L min}^{-1}$ )	15
Sampling period (s)	0.3
Repetitions 3	3
Sample uptake rate ( $\text{mL min}^{-1}$ )	0.4
Integration time (s)	0.1

#### 2.3.4. Shotgun Proteomics Analysis

Shotgun proteomics was performed to assess the protein composition of sample containing 1 million cyanobacteria isolated by instrumental sorting from samples collected in the Lama dei Peligni area. The biological sample was concentrated with 30 KDa filters (Amicon® Ultra, Merck Millipore (Burlington, MA, USA)) and was lysed by sonication on ice (Sonicator U200S control, IKA Labortechnik, Staufen, Germany) at cycle 0.4 and 40% amplitude in a lysis buffer (urea 6 M in 100 mM Tris/HCl, pH = 7.5). Protein concentration was determined using the Bradford assay (Bio-Rad, Hercules, CA, USA) with Bovine Serum Albumin (BSA, Sigma-Aldrich, St. Louis, MI, USA) as the standard for the calibration curve, allowing digestion of 50  $\mu\text{g}$  of protein of sample. Filter-Aided Sample Preparation (FASP) protocol was used for overnight tryptic digestion at 37 °C. The sample was analyzed in triplicate by injecting 3  $\mu\text{L}$  of digested proteins by nano LC-MS/MS through Ultimate™ 3000 UPLC (Thermo Fisher Scientific, Milan, Italy) chromatographic system coupled to the Orbitrap Fusion™ Tribrid™ (Thermo Fisher Scientific, Milan, Italy) mass spectrometer, using the column Easyspray PEPMAP RSLC C18 2  $\mu\text{m}$ , 25 cm  $\times$  75  $\mu\text{m}$  (Thermo Fisher Scientific, Milan, Italy). The sample was acquired with a flow rate set at 300 nL/min and a total run time of 65 min, employing a chromatographic gradient increasing from 5% to 90% of phase B (mobile phase A: 0.1% formic acid in water; mobile phase B: 0.1% formic acid in acetonitrile). The MS parameters and acquisitions were previously described in two works [52,53] used in mass spectrometry employ the high-energy collision-induced dissociation (HCD) technique, which enables the fragmentation of selected molecular ions during acquisition. The MS/MS raw data were processed using Proteome Discoverer 2.5 software (Thermo Fisher Scientific, Milan, Italy), through the “All Entries” reviewed database (25,252 entries, released in 2021, UniProtKB/SwissProt) and Cyanobacteriota/Melainabacteria group (id: 1798711) (3578 entries, released in 2024, UniProtKB/SwissProt) with a false positive rate (FDR) of 1% at protein level for both search engines. For the protein identification, the

following processing filters were applied: all reported proteins were identified as “master proteins” and, additionally, a high confidence threshold was set, including in the dataset only proteins that were present with high confidence in at least 2 out of 3 analytical replicates. Functional enrichment and pathway analysis were performed using STRING version 12 (Search Tool for the Retrieval of Interacting Genes/Proteins) software, a bioinformatics tool used to explore protein–protein interactions based on functional relationships. *p*-values of functional networks were corrected for multiple testing within each category using the Benjamini–Hochberg procedure.

### 3. Results

Microorganism, obtained by resuspending the material collected from the rock paintings in 1X PBS, were analyzed by flow cytometry. As shown in Figure 6, a population of cells was identified in the side scatter height (SSC-H) versus forward scatter height (FSC-H) dot plot (“Morph” gate, Figure 6a), using a 1X PBS sample as a negative control (Figure 6d,e). This population, containing a discrete amount of DNA (Figure 6b,c), as indicated by the histogram shown in Figure 6b, where the blue peak represents the sample stained with SYTO9, while the red peak corresponds to its respective fluorescence minus one (FMO) control. Such a population of cells, obtained from an area of the painting covered by the biofilm, exhibited fluorescence in the Alexa Fluor 647 channel (Figure 6e), consistent with cyanobacterial pigment emission. A sample obtained from a painting control area (not covered by the biofilm) was used as a control (Figure 6d). The sequencing performed with the 16S Metagenomics Kit revealed an important result. Using the Ion Reporter Software (<https://ionreporter.thermofisher.com/ir/>, accessed on 26 October 2025) with the Krona Software, we analyzed all the phylogenetic classes, starting from the major phyla. In particular, in sample 1 (Figure 7), the phylum cyanobacteria revealed 18% of the entire microbial population, with 32,271 total reads, while in sample 2 (Figure 8), cyanobacteria was found only with 3% with 5948 total reads. The multi-elemental concentrations detected in the different samples are listed in Table 2. The main differences between moss and blackened moss shed light on probable presence by heavy metals (Pb, Cd, Zn and Mn) especially of the blackened samples. These data may confirm the colonization of cyanobacteria in areas where the moss appears blackened, possibly due to heavy metal stressors acting as a selective pressure. Statistical differences were evaluated with two-way ANOVA test and, then, to control the false discovery rate (FDR), we applied the two-stage linear step-up procedure of Benjamini, Krieger, and Yekutieli (BKY) by reporting the *p*-values in Supplementary Materials Table S1. As the Majella Massif hosts prehistoric rock art now threatened by microbial colonization, we performed proteomics analysis on cyanobacteria isolated by FACS. Comparing the searches through two databases, 22 proteins were robustly identified (9.44%) with respect to the “All entries” database reclassified as Cyanobacteriota phylum, as shown in the Venn diagram in Figure 9. When research was reduced to only Cyanobacteriota phylum, 33 proteins were reclassified in the Cyanobacteriota/Melainabacteria group. Of them, 22 proteins were the same as the previous identification in the “All entries” database. Most of the identified proteins were reclassified to the species *Nostoc punctiforme*, a filamentous cyanobacterium characterized as one of the most active inteins, as demonstrated by the number of peptides with which they have been identified because it is greater than the proteins reclassified with other species of cyanobacteria. We studied the PPI of these 33 proteins in order to visualize functional protein clusters, as shown in Figure 10a,b, demonstrating that they are involved in photosynthesis and ATP metabolism. The whole protein list is reported in the Supplementary Materials Table S2.

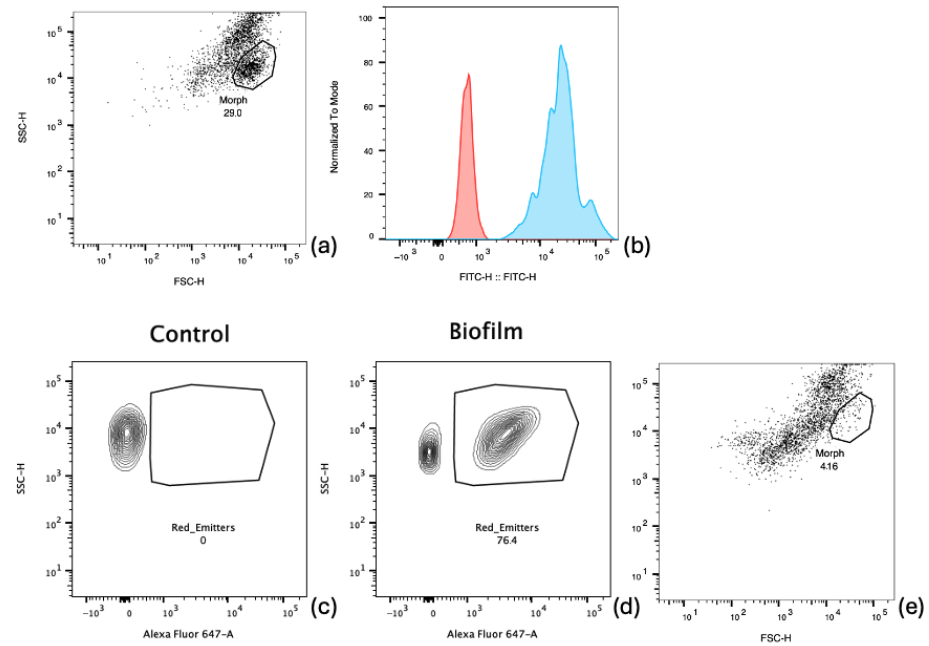


**Figure 6.** Identification of microbial populations from rock painting samples by flow cytometry. Microorganisms resuspended in 1X PBS from rock painting swabs were analyzed by flow cytometry. (a) A distinct population was identified in a side scatter height (SSC-H) vs. forward scatter height (FSC-H) dot plot. (b) The whole identified population was analyzed for SYTO9 staining. The blue peak represents the SYTO9-stained population, while the red peak corresponds to the related fluorescence minus one (FMO) control. (c) The identified SYTO9+ population of cells was represented on a SSC-H vs. Alexa Fluor 647-H contour plot. The Alexa Fluor 647 channel (660/20 nm) is well suited for detecting cyanobacteria-specific fluorescence (emission peak around 650–660 nm). The same analytical representation was applied to both a sample collected from a control area of the painting (not covered by biofilm), used as a negative control (c), and to the SYTO9+ population obtained from a biofilm-covered region of the painting (d). (e) 1X PBS alone was analyzed as an additional negative control to exclude background on scatter signals. Data are representative of three independent experiments.

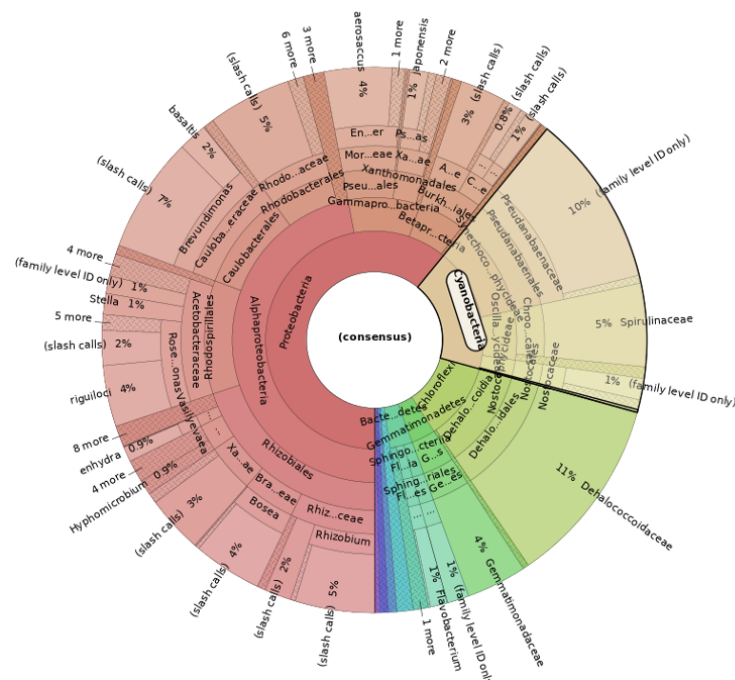


**Figure 7.** Output referred to sample 1.

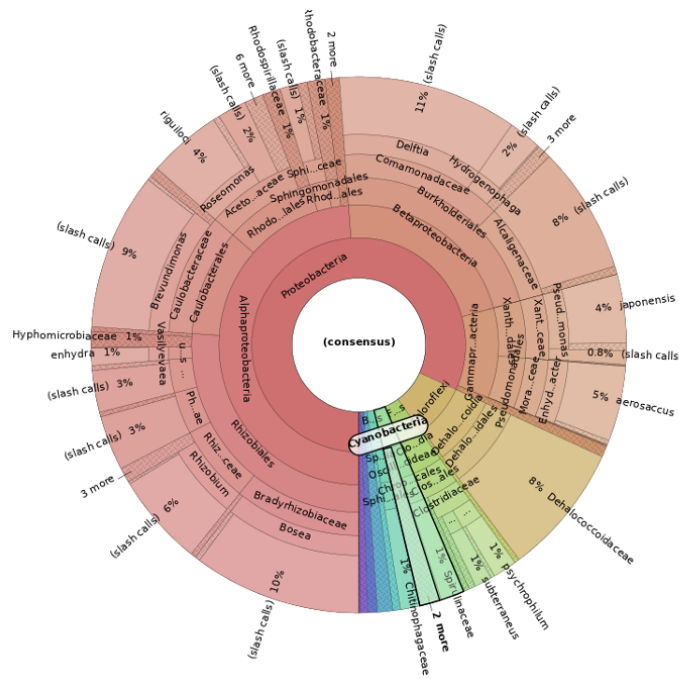


Figure 8. Output referred to sample 2.

Table 2. Elemental composition of the samples (ng mL<sup>-1</sup> ± relative standard deviation (n = 3)). In the table, the main differences between blackened moss and only moss are highlighted in bold. \* Values fall outside the calibration curve used. \*\* Values are below the limit of quantification and identified with N/A in the table below.

MOSS	BLACKENED MOSS	SOIL	ROCK SURFACE
Co = 6.6 ± 0.2	Co = 2.9 ± 1	Co = 12.9 ± 5.7	Co = 3.8 ± 2.7
Cr = 2.2 ± 2.9	Cr = 5.6 ± 2.2	Cr = 1.5 ± 6.5	Cr = 11.7 ± 4.7
Al = 713.3 * ± 8.4	<b>Al = 3329.3 * ± 0.7</b>	Al = 435.2 * ± 1.7	Al = 1532.3 * ± 2.4
Ag = N/A **	Ag = 0.23 ± 4.7	Ag = N/A **	Ag = N/A **
As = 4.4 ± 5.1	As = 2.01 ± 1.9	As = 4.8 ± 0.6	As = 12.6 ± 4.2
Cd = 0.13 ± 3.4	<b>Cd = 5.4 ± 1.7</b>	Cd = 0.18 ± 10.9	Cd = 624.2 * ± 1.3
Cu = 16.9 ± 6.7	Cu = 19.3 ± 2.3	Cu = 16.2 ± 1	Cu = 42.2 ± 3.1
Mn = 25.2 ± 7.2	<b>Mn = 115.5 * ± 0.6</b>	Mn = 17.7 ± 1.7	Mn = 188.4 * ± 2.7
Ni = 56.3 ± 0.1	Ni = 12.9 ± 0.9	Ni = 107 ± 6.5	Ni = 41.4 ± 8.7
Pb = 1.9 ± 8.6	<b>Pb = 255.6 ± 4.9</b>	Pb = 1.4 ± 1	Pb = 24.8 ± 6.9
Se = 1.8 ± 13.4	<b>Se = 11.5 ± 7.2</b>	Se = 3.2 ± 16	Se = 18 ± 6.9
V = 11.7 ± 7	V = 6.9 ± 0.8	V = 12.1 ± 0.5	V = 23.31 ± 1.6
Zn = 17.9 ± 7.1	<b>Zn = 54.7 ± 1.7</b>	Zn = 22.2 ± 1.1	Zn = 82.9 ± 3.1

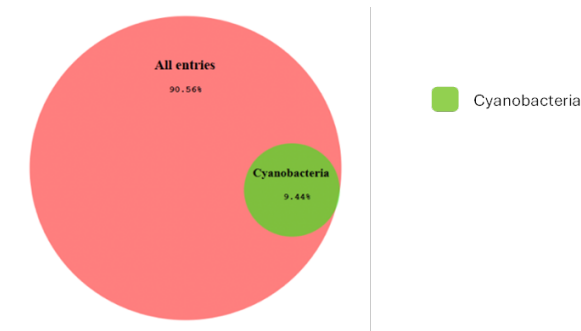


Figure 9. Venn diagram showing the percentage of protein identified through Cyanobacteria/Melainabacteria group (in green) related to the various species derived from the 'All Entries' database of UniProtKB/SwissProt.



enhanced stress resilience. Such metal enrichment has been associated with shifts in lithic microbiomes and with black crust formation patterns used as markers of environmental change on heritage limestones [16,40]. While causality cannot be inferred from our cross-sectional data, the co-occurrence of higher temperature signals and metal loadings points to multi-stressor scenarios in which warming and pollutant availability jointly facilitate colonization and persistence.

From a conservation standpoint, these findings underscore the need to integrate climate indicators into routine diagnostic and preventative strategies for open-air rock art. First, site-based microclimate monitoring (temperature, RH, wetting/drying frequency, irradiance) should be coupled with periodic, minimally invasive microbiological assessments (e.g., qPCR or metabarcoding panels targeting cyanobacteria) to detect early deviations towards higher bioreceptivity states [19]. Second, given the environmental and regulatory concerns around repeated use of broad-spectrum biocides, the evaluation of lower-impact control options (e.g., essential oils or other nature-based antimicrobials, photodynamic or photocatalytic treatments, and cleaning protocols tuned to local bioreceptivity) is warranted [35,36]. These interventions should be framed within adaptive management plans that account for seasonal windows of highest biofilm activity and the specific geometry and shading of decorated shelters, known determinants of colonization intensity [19,28].

This work has limitations. Laboratory growth was assessed at two discrete temperatures without full replication across a gradient, and no formal hypothesis testing was applied to the cfu differences. Moreover, other key drivers (light spectrum/intensity, surface moisture dynamics, nutrient availability, and wind-driven rain) were not manipulated experimentally and may modulate the temperature response in situ [46,47]. In summary, our interdisciplinary evidence indicates that recent warming conditions are consistent with enhanced cyanobacterial activity on the Lama dei Peligni rock paintings, reinforcing concerns that climate change can accelerate biodeterioration in Mediterranean open-air heritage. Translating these insights into practice will require climate-informed monitoring, targeted and sustainable biocontrol trials, and site-specific risk models that jointly consider climate trends, pollutant loads and substrate bioreceptivity.

## 5. Conclusions

This study provides converging evidence that recent warming consistent with regional climate change can enhance cyanobacterial proliferation on lithic substrates at the Lama dei Peligni rock art site (Majella Massif, Italy). Integrating atmospheric records with microbiological, chemical and proteomic analyses, we showed that higher temperatures are associated with increased cyanobacterial growth, metabolically active biofilms (with proteins largely assigned to *Nostoc punctiforme*), and co-occurring elemental patterns suggestive of metal-related selective pressures. Even modest laboratory differences in growth at 18.6 °C versus 14.3 °C may translate, in situ, into thicker and more persistent subaerial biofilms that obscure pigments and accelerate chemical and mechanical decay of painted surfaces.

Our findings support the urgent incorporation of climate indicators into conservation diagnostics and preventative management for open-air rock art in Mediterranean settings. We recommend (i) site-specific microclimate monitoring linked to periodic, minimally invasive microbiome assessments; (ii) evaluation of lower-impact biocontrol options as alternatives or complements to synthetic biocides; and (iii) scheduling interventions around seasonal windows of peak bioreceptivity.

Future work should expand experimental designs to multi-factor gradients (temperature, irradiance, wetting/drying) and couple proteogenomic surveys with high-resolution imaging of paint layers to quantify aesthetic and material outcomes through time. Such

climate-informed, interdisciplinary approaches are essential to mitigate the escalating biodegradation risks posed by cyanobacterial colonization to vulnerable cultural heritage sites.

**Supplementary Materials:** The following supporting information can be downloaded at: <https://www.mdpi.com/article/10.3390/su172310861/s1>, Table S1: *p*-value for each analyzed element. Table S2: List of quantified proteins.

**Author Contributions:** Conceptualization, P.C., F.P., E.M.S., E.A., S.D., P.D.C. and A.M.; methodology, P.C., F.P., E.M.S., E.A., S.D., P.D.C. and A.M.; formal analysis, P.C., P.S., P.L., S.D.L., M.D.G., S.G., P.D.B., G.S., M.C.C., V.G., F.A. and A.M.; data curation, P.C., P.S., P.L., S.D.L., M.D.G., S.G., P.D.B., G.S., M.C.C., V.G., F.A. and A.M.; writing—original draft preparation, P.C., F.P., E.M.S., E.A., P.S., P.L., S.D.L., M.D.G., S.G., P.D.B., M.C.C., V.G., F.A., S.D., P.D.C. and A.M.; writing—review and editing, P.C., F.P., E.M.S., E.A., C.A., S.D., P.D.C. and A.M.; supervision, P.C., F.P., C.A., S.D., P.D.C. and A.M. All authors have read and agreed to the published version of the manuscript.

**Funding:** This research was funded by the European Union NextGenerationEU, under the National Recovery and Resilience Plan (NRRP), Mission 4 Component 2-M4C2, Investment 1.5 Call for tender No. 3277 of 30 December 2021, Italian Ministry of University, Award Number: ECS00000041, Project Title: “Innovation, digitalization, and sustainability for the diffused economy in Central Italy”, Concession Degree No. 1057 of 23 June 2022 adopted by the Italian Ministry of University. CUP: D73C22000840006. Alessandra Mascitelli, Piero Chiacchiarretta, Eleonora Aruffo and Piero Di Carlo acknowledge financial support funded by the European Union NextGenerationEU.

**Institutional Review Board Statement:** Not applicable.

**Informed Consent Statement:** Not applicable.

**Data Availability Statement:** The original contributions presented in this study are included in the article/supplementary material. Further inquiries can be directed to the corresponding author.

**Acknowledgments:** The authors would like to acknowledge the cooperation and availability of the Maiella National Park President, Lucio Zazzera, the Maiella National Park Director, Luciano Di Martino, and President of the Castel di Sangro Section of the Alpine Club, Franco D’Ambrosio

**Conflicts of Interest:** The authors declare no conflicts of interest.

## References

- Palmerini, G. *L’arte Rupestre nel Parco Nazionale Della Maiella. Ricerche Storiche, Indagini in Corso e Nuove Prospettive*; Ente Parco Nazionale della Maiella: Abruzzo, Italy, 2023.
- Mattioli, T. *L’arte Rupestre in Italia Centrale: Umbria, Lazio, Abruzzo*; Ali&No: Perugia, Italy, 2007; Volume 4.
- Palmerini, G.; Beck, L.; Di Martino, L.; Gallet, X.; Lebon, M.; Manzi, A.; Nicoud, E.; Mariano, A.; Villa, V. # MaiellaRockArtProject: Nuove ricerche sull’arte rupestre dell’Appennino abruzzese. In Proceedings of the XXVIII Valcamonica Symposium: ROCK-ART, A HUMAN HERITAGE, Valcamonica, Italy, 28–31 October 2021; Centro Camuno di Studi Preistorici: Capo di Ponte, Italy, 2021.
- Di Fraia, T. Le nuove scoperte di arte rupestre in Abruzzo: Verso un’interpretazione sistemica. *L’RTE RUPESTRE* **2015**. Available online: [https://www.researchgate.net/publication/354836318\\_Le\\_nuove\\_scoperte\\_di\\_arte\\_rupestre\\_in\\_Abruzzo\\_verso\\_un\\_interpretazione\\_sistemica](https://www.researchgate.net/publication/354836318_Le_nuove_scoperte_di_arte_rupestre_in_Abruzzo_verso_un_interpretazione_sistemica) (accessed on 26 October 2025).
- Mattioli, T. Landscape analysis of a sample of rock-art sites in Central Italy. In Proceedings of the Layers of Perception: Proceedings of the 35th International Conference on Computer Applications and Quantitative Methods in Archaeology (CAA), Berlin, Germany, 2–6 April 2007; pp. 342–343.
- Nuhoglu, Y.; Oguz, E.; Uslu, H.; Ozbek, A.; Ipekoglu, B.; Ocak, I.; Hasenekoglu, I. The accelerating effects of the microorganisms on biodeterioration of stone monuments under air pollution and continental-cold climatic conditions in Erzurum, Turkey. *Sci. Total Environ.* **2006**, *364*, 272–283. [[CrossRef](#)] [[PubMed](#)]
- Kumar, R.; Kumar, A.V. *Biodeterioration of Stone in Tropical Environments: An Overview*; The Getty Conservation Institute: Los Angeles, CA, USA, 1999.
- Ortega-Morales, B.O.; Gaylarde, C.C.; Englert, G.E.; Gaylarde, P.M. Analysis of salt-containing biofilms on limestone buildings of the Mayan culture at Edzna, Mexico. *Geomicrobiol. J.* **2005**, *22*, 261–268. [[CrossRef](#)]
- Tomaselli, L.; Lamenti, G.; Bosco, M.; Tiano, P. Biodiversity of photosynthetic micro-organisms dwelling on stone monuments. *Int. Biodeterior. Biodegrad.* **2000**, *46*, 251–258. [[CrossRef](#)]

10. Gaylarde, P.M.; Gaylarde, C.C. Algae and cyanobacteria on painted buildings in Latin America. *Int. Biodeterior. Biodegrad.* **2000**, *46*, 93–97. [[CrossRef](#)]
11. Crispim, C.A.; Gaylarde, C. Cyanobacteria and biodeterioration of cultural heritage: A review. *Microb. Ecol.* **2005**, *49*, 1–9. [[CrossRef](#)]
12. Zanardini, E.; Abbruscato, P.; Ghedini, N.; Realini, M.; Sorlini, C. Influence of atmospheric pollutants on the biodeterioration of stone. *Int. Biodeterior. Biodegrad.* **2000**, *45*, 35–42. [[CrossRef](#)]
13. Warscheid, T.; Braams, J. Biodeterioration of stone: A review. *Int. Biodeterior. Biodegrad.* **2000**, *46*, 343–368. [[CrossRef](#)]
14. Scheerer, S.; Ortega-Morales, O.; Gaylarde, C. Microbial deterioration of stone monuments—An updated overview. *Adv. Appl. Microbiol.* **2009**, *66*, 97–139.
15. Ortega-Morales, O.; Montero-Muñoz, J.L.; Neto, J.A.B.; Beech, I.B.; Sunner, J.; Gaylarde, C. Deterioration and microbial colonization of cultural heritage stone buildings in polluted and unpolluted tropical and subtropical climates: A meta-analysis. *Int. Biodeterior. Biodegrad.* **2019**, *143*, 104734. [[CrossRef](#)]
16. Louati, M.; Ennis, N.J.; Ghodhbane-Gtari, F.; Hezbri, K.; Sevigny, J.L.; Fahnestock, M.F.; Cherif-Silini, H.; Bryce, J.G.; Tisa, L.S.; Gtari, M. Elucidating the ecological networks in stone-dwelling microbiomes. *Environ. Microbiol.* **2020**, *22*, 1467–1480. [[CrossRef](#)]
17. Sesana, E.; Gagnon, A.S.; Ciantelli, C.; Cassar, J.; Hughes, J.J. Climate change impacts on cultural heritage: A literature review. *Wiley Interdiscip. Rev. Clim. Change* **2021**, *12*, e710. [[CrossRef](#)]
18. Gu, J.D.; Katayama, Y. Microbiota and biochemical processes involved in biodeterioration of cultural heritage and protection. *Microorg. Deterior. Preserv. Cult. Herit.* **2021**, *37*, 37–58.
19. Macedo, M.F.; Miller, A.Z.; Dionísio, A.; Saiz-Jimenez, C. Biodiversity of cyanobacteria and green algae on monuments in the Mediterranean Basin: An overview. *Microbiology* **2009**, *155*, 3476–3490. [[CrossRef](#)] [[PubMed](#)]
20. Urzì, C.; Realini, M. Colour changes of Notos calcareous sandstone as related to its colonisation by microorganisms. *Int. Biodeterior. Biodegrad.* **1998**, *42*, 45–54. [[CrossRef](#)]
21. Gambino, M.; Sanmartín, P.; Longoni, M.; Villa, F.; Mitchell, R.; Cappitelli, F. Surface colour: An overlooked aspect in the study of cyanobacterial biofilm formation. *Sci. Total Environ.* **2019**, *659*, 342–353. [[CrossRef](#)]
22. Ortega-Morales, O.; Guezenec, J.; Hernandez-Duque, G.; Gaylarde, C.C.; Gaylarde, P.M. Phototrophic biofilms on ancient Mayan buildings in Yucatan, Mexico. *Curr. Microbiol.* **2000**, *40*, 81–85. [[CrossRef](#)]
23. Gorbushina, A.A. Life on the rocks. *Environ. Microbiol.* **2007**, *9*, 1613–1631. [[CrossRef](#)]
24. Guillitte, O. Bioreceptivity: A new concept for building ecology studies. *Sci. Total Environ.* **1995**, *167*, 215–220. [[CrossRef](#)]
25. Sanmartín, P.; Miller, A.; Prieto, B.; Viles, H.A. Revisiting and reanalysing the concept of bioreceptivity 25 years on. *Sci. Total Environ.* **2021**, *770*, 145314. [[CrossRef](#)]
26. Miller, A.; Sanmartín, P.; Pereira-Pardo, L.; Dionísio, A.; Sáiz-Jiménez, C.; Macedo, M.; Prieto, B. Bioreceptivity of building stones: A review. *Sci. Total Environ.* **2012**, *426*, 1–12. [[CrossRef](#)]
27. Viles, H.; Ahmad, H. Architectural controls on the bioreceptivity of sandstone to green algal colonization. ECBSM2016. In Proceedings of the European Conference on Biodeterioration of Stone Monuments-Second Edition, Cergy-Pontoise, France, 17–18 November 2016.
28. Cattò, C.; Mu, A.; Moreau, J.W.; Wang, N.; Cappitelli, F.; Strugnelli, R. Biofilm colonization of stone materials from an Australian outdoor sculpture: Importance of geometry and exposure. *J. Environ. Manag.* **2023**, *339*, 117948. [[CrossRef](#)] [[PubMed](#)]
29. Trovão, J.; Portugal, A. The impact of stone position and location on the microbiome of a marble statue. *Microbe* **2024**, *2*, 100040. [[CrossRef](#)]
30. Ohkubo, S.; Miyashita, H. A niche for cyanobacteria producing chlorophyll f within a microbial mat. *ISME J.* **2017**, *11*, 2368–2378. [[CrossRef](#)] [[PubMed](#)]
31. Fiedler, B.; Broc, D.; Schubert, H.; Rediger, A.; Börner, T.; Wilde, A. Involvement of Cyanobacterial Phytochromes in Growth Under Different Light Qualities and Quantities. *Photochem. Photobiol.* **2004**, *79*, 551–555. [[CrossRef](#)]
32. Liu, X.; Qian, Y.; Wu, F.; Wang, Y.; Wang, W.; Gu, J.D. Biofilms on stone monuments: Biodeterioration or bioprotection? *Trends Microbiol.* **2022**, *30*, 816–819. [[CrossRef](#)]
33. Favero-Longo, S.E.; Viles, H.A. A review of the nature, role and control of lithobionts on stone cultural heritage: Weighing-up and managing biodeterioration and bioprotection. *World J. Microbiol. Biotechnol.* **2020**, *36*, 100. [[CrossRef](#)]
34. Pinna, D. *Coping with Biological Growth on Stone Heritage Objects: Methods, Products, Applications, and Perspectives*; Apple Academic Press: Burlington, ON, USA, 2017.
35. Cappitelli, F.; Cattò, C.; Villa, F. The control of cultural heritage microbial deterioration. *Microorganisms* **2020**, *8*, 1542. [[CrossRef](#)]
36. Macchia, A.; Aureli, H.; Prestileo, F.; Ortenzi, F.; Sellathurai, S.; Docci, A.; Cerafogli, E.; Colasanti, I.A.; Ricca, M.; La Russa, M.F. In-situ comparative study of eucalyptus, basil, cloves, thyme, pine tree, and tea tree essential oil biocide efficacy. *Methods Protoc.* **2022**, *5*, 37. [[CrossRef](#)]
37. Angelova, B.; Traykov, I.; Boteva, S.; Tsvetkov, M.; Kenarova, A. Bacterial Metabolic Activity of High-Mountain Lakes in a Context of Increasing Regional Temperature. *Microorganisms* **2025**, *13*, 1375. [[CrossRef](#)]

38. Gaylarde, C.C. Influence of environment on microbial colonization of historic stone buildings with emphasis on cyanobacteria. *Heritage* **2020**, *3*, 1469–1482. [[CrossRef](#)]
39. May, E.; Papida, S.; Abdulla, H.; Tayler, S.; Dewedar, A. Comparative studies of microbial communities on stone monuments in temperate and semi-arid climates. In *Of Microbes and Art: The Role of Microbial Communities in the Degradation and Protection of Cultural Heritage*; Springer: Berlin/Heidelberg, Germany, 2000; pp. 49–62.
40. Perez-Monserrat, E.M.; Varas-Muriel, M.J.; Alvarez De Buergo, M.; Fort, R. Black layers of decay and color patterns on heritage limestone as markers of environmental change. *Geosciences* **2016**, *6*, 4. [[CrossRef](#)]
41. Chen, X.; Bai, F.; Huang, J.; Lu, Y.; Wu, Y.; Yu, J.; Bai, S. The organisms on rock cultural heritages: Growth and weathering. *Geoheritage* **2021**, *13*, 56. [[CrossRef](#)]
42. Ding, X.; Lan, W.; Yan, A.; Li, Y.; Katayama, Y.; Gu, J.D. Microbiome characteristics and the key biochemical reactions identified on stone world cultural heritage under different climate conditions. *J. Environ. Manag.* **2022**, *302*, 114041. [[CrossRef](#)] [[PubMed](#)]
43. Wang, C.; Wang, L.; Bai, C.; Wang, M.; Ma, T.; Ma, H.; Zhang, G.; Wang, W.; Guo, Z.; Sun, Y.; et al. Identification of the key factors influencing biodeterioration of open-air cultural heritage in the temperate climate zone of China. *Int. Biodeterior. Biodegrad.* **2025**, *196*, 105954. [[CrossRef](#)]
44. American Society for Microbiology. *Microbes and Climate Change-Science, People & Impacts: Report on an American Academy of Microbiology Virtual Colloquium held on Nov. 5, 2021*; American Society for Microbiology: Washington, DC, USA, 2022.
45. Viles, H.A.; Cutler, N.A. Global environmental change and the biology of heritage structures. *Glob. Change Biol.* **2012**, *18*, 2406–2418. [[CrossRef](#)]
46. Traversetti, L.; Bartoli, F.; Caneva, G. Wind-driven rain as a bioclimatic factor affecting the biological colonization at the archaeological site of Pompeii, Italy. *Int. Biodeterior. Biodegrad.* **2018**, *134*, 31–38. [[CrossRef](#)]
47. Orr, S.A.; Cassar, M. Exposure indices of extreme wind-driven rain events for built heritage. *Atmosphere* **2020**, *11*, 163. [[CrossRef](#)]
48. Albertano, P. Cyanobacterial biofilms in monuments and caves. In *Ecology of Cyanobacteria II: Their Diversity in Space and Time*; Springer: Berlin/Heidelberg, Germany, 2012; pp. 317–343.
49. Drugă, B.; Ramm, E.; Szekeres, E.; Chiriac, C.; Hegedüs, A.; Stockenreiter, M. Long-term acclimation might enhance the growth and competitive ability of *Microcystis aeruginosa* in warm environments. *Freshw. Biol.* **2022**, *67*, 589–602. [[CrossRef](#)]
50. Olsson-Francis, K.; de la Torre, R.; Cockell, C.S. Isolation of novel extreme-tolerant cyanobacteria from a rock-dwelling microbial community by using exposure to low Earth orbit. *Appl. Environ. Microbiol.* **2010**, *76*, 2115–2121. [[CrossRef](#)]
51. Chiaudani, A.; Flamminii, F.; Consalvo, A.; Bellocchi, M.; Pizzi, A.; Passamonti, C.; Cichelli, A. Rare Earth Element Variability in Italian Extra Virgin Olive Oils from Abruzzo Region. *Foods* **2024**, *13*, 141. [[CrossRef](#)]
52. Potenza, F.; Cufaro, M.C.; Di Biase, L.; Panella, V.; Di Campli, A.; Ruggieri, A.G.; Dufrusine, B.; Restelli, E.; Pietrangelo, L.; Protasi, F.; et al. Proteomic analysis of marinesco–sjogren syndrome fibroblasts indicates pro-survival metabolic adaptation to SIL1 loss. *Int. J. Mol. Sci.* **2021**, *22*, 12449. [[CrossRef](#)]
53. Ucci, A.; Giacchi, L.; Cufaro, M.C.; Puri, C.; Ciocca, M.; Di Ferdinando, F.; Del Boccio, P.; Cappariello, A.; Rucci, N. Human osteosarcoma cell secretome impairs neonatal mouse calvarial osteogenic cells functions and modifies the nanoparticles-derived protein profile. *Life Sci.* **2025**, *379*, 123837. [[CrossRef](#)]

**Disclaimer/Publisher’s Note:** The statements, opinions and data contained in all publications are solely those of the individual author(s) and contributor(s) and not of MDPI and/or the editor(s). MDPI and/or the editor(s) disclaim responsibility for any injury to people or property resulting from any ideas, methods, instructions or products referred to in the content.